Available online at www.sciencedirect.com

SCIENCE DIRECT

Thermochimica Acta 409 (2004) 19–24

thermochimica acta

www.elsevier.com/locate/tca

Thermochemistry of adducts of some transition metals(II) bromides with pyridine N-oxide

Pedro Oliver Dunstan*

Instituto de Química, Universidade Estadual de Campinas, C.P. 6154, CEP 13083-862, Campinas, São Paulo, Brazil

Received 29 January 2003; received in revised form 29 May 2003; accepted 30 May 2003

Abstract

The compounds $[MBr_2(pyNO)_n]$ (where M: Mn, Fe, Co, Ni, Cu or Zn; pyNO is pyridine N-oxide and $n = 2$, 3 or 6) were synthesized and characterized by melting points, elemental analysis, thermal analysis and electronic and IR spectroscopy. The enthalpies of dissolution of the adducts, metal(II) bromides and pyNo in methanol were measured and by using thermochemical cycles, the following thermochemical parameters for the adducts have been determined: the standard enthalpies for the Lewis acid/base reactions ($\Delta_r H^\theta$), the standard enthalpies of formation ($\Delta_f H^\theta$), the standard enthalpies of decomposition ($\Delta_D H^\theta$), the lattice standard enthalpies ($\Delta_M H^\theta$) and the standard enthalpies of the Lewis acid/base reactions in the gaseous phase ($\Delta_r H^\theta(g)$). The mean bond dissociation enthalpies of the M(II)–oxygen bonds ($\bar{D}_{(M–O)}$) have been estimated.

Keywords: Metal(II) bromides; Transition metals; Thermochemistry; Metal(II)–oxygen bonds; Dissolution enthalpies

1. Introduction

The synthesis of complexes of divalent 3*d* electrons elements with pyridine N-oxide is found in the literature [1–3]. However, no information about the enthalpies of the transition element–oxygen bonds formed in these compounds is available. Adducts of bromides of some divalent transition metals of the first series with pyridine N-oxide are synthesized here with the purpose of obtaining the enthalpies involved in the formation of the adducts and to establish correlations between the bond energies and other thermochemical parameters. The ligand field parameters of the adducts were also calculated. The bromides were selected among several other salts because they have thermochemical data cited in the literature [4]. Adducts of pyNO that are not found in the literature were also obtained.

2. Experimental

2.1. Chemicals

Pyridine N-oxide was prepared according to Ochiai's method [5]. All the anhydrous metal(II) bromides used in the preparation of the adducts were of reagent grade.

Solvents used in the synthesis of the adducts and in the calorimetric measurements were purified by distillation and stored over Linde 4 Å molecular sieves.

2.2. Analytical

Carbon, hydrogen and nitrogen contents were determined by microanalytical procedures. The metal contents were determined by complexometric titration with 0.01 M EDTA solution [6] of the aqueous solution of the adduct samples. Bromide analysis was obtained by gravimetry using standard 0.1 M $AgNO_3$ solution, after the adducts had been dissolved in water [7]. The capillary melting points of the adducts were determined using a UNIMELT equipment from Thomas Hover.

2.3. Adducts synthesis

The adducts were prepared by the reaction of ethanolic solutions of the anhydrous metal(II) bromides with ethanolic solutions of the ligand pyNO. A typical procedure is given bellow.

To a solution of 1.0 g of $CoBr_2$ (4.6 mmol) in 65 ml of dry ethanol, 2.6 g of pyNO (27.4 mmol) in 60 ml of dry ethanol was slowly added drop-wise under stirring. The solid formed was filtered and washed with petroleum ether. The product was dried for several hours in vacuum and stored in

---

* Tel.: +55-19-788-3088; fax: +55-19-788-3023.
E-mail address: dunstan@iqm.unicamp.br (P.O. Dunstan).

0040-6031/$ – see front matter © 2003 Elsevier B.V. All rights reserved.
doi:10.1016/S0040-6031(03)00333-2

a desiccator over calcium chloride. In all cases it was used a molar ratio acceptor/donator of 1:6.

2.4. Infrared spectra

Spectra were obtained with samples in KBr matrix for the adducts and ligand. A Perkin-Elmer 1600 series FT-IR spectrophotometer in the 4000–400 cm^{-1} region was used.

2.5. Thermal studies

TG/DTG and DSC measurements were obtained in argon atmosphere in a Du Pont 951 TG analyzer with the samples varying in mass from 9.22 to 13.22 mg (TG/DTG) and from 6.55 to 7.61 mg (DSC) and a heating rate of 10 K min^{-1} in the 293–673 K (DSC) and 298–1173 K (TG/DTG) temperature ranges. TG calibration for temperatures was made using metallic aluminum as standard (mp=660.37 °C) and the equipment carried out the calibration for mass automatically. The DSC calibration was made using metallic indium as standard (mp =165.73 °C, $\Delta_s^1 H^\theta = 28.4\,\text{J g}^{-1}$).

2.6. Calorimetric measurements

All the solution calorimetric measurements were carried out in an LKB 8700-1 precision calorimeter as described elsewhere [8]. The solution calorimetric measurements were performed by dissolving samples of 3.6–111.5 mg of the adducts or metal bromides in 100 ml of methanol and the ligand pyNO in this latter solution, maintaining a molar relation equal to the stoichiometry of the adduct. The accuracy of the calorimeter was carried out by determining the heat of dissolution of tris((hydroxymethyl)amino)methane in 0.1 mol dm^{-3} HCl. The result ($-29.78 \pm 0.03\,\text{kJ mol}^{-1}$) is in agreement with the value recommended by IUPAC ($-29.763 \pm 0.003\,\text{kJ mol}^{-1}$) [9].

2.7. Electronic spectra

Spectra in the 350–2000 nm region were obtained with a UV-Vis-NIR Varian-Cary 5 G spectrophotometer, with a standard reflectance attachment for obtaining the spectra of the solid adducts.

3. Results and discussion

All adducts obtained were solids. The yields ranged from 59 to 88%. The yields, melting points, colors, appearance and analytical data are summarized in Table 1.

3.1. Infrared spectra

The infrared spectra of pyNO adducts showed a small shift, splitting or decrease in intensity of some bands when compared with the spectrum of free pyNO. Coordinated pyNO is distinguished from free pyNO by a decrease in the frequency of the NO stretching vibration (at 1243 cm^{-1} in free pyNO) upon coordination [10–12]. The infrared spectral data, used in characterize the compounds studied, is available from the author upon request.

3.2. Thermal analysis

Thermogravimetry and derivative thermogravimetry of the adducts show the associated thermal dissociation process of different types, losing part of the ligand, all the ligand or all the ligand and part of the salt in a first step of mass lost. This first step consists of one, two, three or five successive processes. The intermediate products lost the rest of the ligand and part of the salt in a second step, with exception of the adduct of Mn(II) that lost mass in more two steps. These latter steps also consist of one, two or three successive processes, leaving a residue that is probably the respective metal.

The DSC curves of the adducts are consistent with the TG/DTG data and show endothermic peaks due to the partial elimination of ligand or elimination of all the ligand and part of the CuBr_2 in the case of the adduct $[\text{CuBr}_2(\text{pyNO})_2]$. Table 2 lists the thermoanalytical data of the adducts.

3.3. Electronic spectra

Table 3 contains the band maxima assignments and calculated ligand field parameters for the adducts. The ligand field parameters for the Ni(II) adduct were calculated according to Reedijk et al. [13] and Lever [14]. According to the number and position of the observed bands and considering the

Table 1
Yields in % on preparation, melting points, appearance and analytical data of the adducts

Compound	Yield	Melting point (K)[a]	Appearance[b]	C		H		N		M		Br	
				Calcd.	Found	Calcd.	Found	Calcd.	Found	Calcd.	Found	Calcd.	Found
$[\text{MnBr}_2(\text{pyNO})_3]$	69	188–189	ye. crs.	36.33	36.11	3.02	3.10	8.40	8.33	10.99	11.12	31.96	32.00
$[\text{FeBr}_2(\text{pyNO})_3]$	59	72–73[a]	re. br. pw.	36.23	35.99	3.02	2.98	8.38	8.32	11.15	11.20	31.90	31.99
$[\text{CoBr}_2(\text{pyNO})_3]_n$	65	210–212[a]	gre. Br. pw.	36.04	35.82	3.00	3.02	8.34	8.40	11.69	11.61	31.71	31.80
$[\text{NiBr}_2(\text{pyNO})_6]$	83	179–180	l. gr. crs.	46.04	45.84	3.83	3.76	10.65	10.50	7.44	7.34	20.25	20.20
$[\text{CuBr}_2(\text{pyNO})_2]$	88	169–170[a]	yel. or. pw.	29.29	29.51	2.44	2.30	6.77	6.83	15.36	15.35	38.64	38.60
$[\text{ZnBr}_2(\text{pyNO})_2]$	83	130–131[a]	wh. pw.	29.16	29.32	2.43	2.41	6.75	6.60	15.72	15.58	38.48	38.38

[a] Melting with decomposition.

[b] Key: l., light; ye., yellow; re., reddish; br., brown; gre., greenish; gr., green; yel., yellowish; or., orange; wh., white; crs., crystals; pw., powder.

Table 2
Thermal analysis data of the compounds

Compound	Mass lost (%)		TG temperature range (K)	Species lost	DSC peak	ΔH^{θ} (kJ mol^{-1})
	Calculated	Observed				
$[MnBr_2(pyNO)_3]$	19.0	19.0[a]	362–470	−pyNO	337	1.79
	38.0	38.2[b]	508–659	−2pyNO	390	1.60
	32.0	32.4[a]	944–1015	$-Br_2$	466	46.98
		8.0[c]				
$[FeBr_2(pyNO)_3]$	70.6	70.6[a]	344–527	$-3pyNO - 3/7Br_2$	334	20.28
	13.7	13.2	913–960	$-3/7Br_2$	391	18.54
		16.2[c]				
$[CoBr_2(pyNO)_3]_n$	56.6	54.7[a]	365–572	−3pyNO	368	0.20
	31.7	39.8[a]	848–1047	$-Br_2$		
		5.42[c]				
$[NiBr_2(pyNO)_6]$	72.3	70.9[d]	433–592	−6pyNO	457	127.68
	20.3	20.4	842–911	$-Br_2$		
		8.8[c]				
$[CuBr_2(pyNO)_2]$	58.9	59.8	475–521	$-2pyNO - 1/6Br_2$	449	25.53
	41.1	39.3	802–892	$-Cu - 1/3Br_2$		
$[ZnBr_2(pyNO)_2]$	95.7	95.6[b]	547–738	$-2pyNO - 0.9ZnBr_2$	368	5.03
	2.7	3.1	738–973	$-0.05ZnBr_2$	402	14.52
		1.7[c]				

[a] Two overlapping peaks of mass lost.
[b] Three overlapping peaks of mass lost.
[c] Residue at 1258 K.
[d] Five overlapping peaks of mass lost.

magnitude of the crystal field parameters as compared with those obtained by Bolster [15], it is concluded that six oxygen atoms from six pyNO molecules octahedrally surround the Ni(II) ion. The diffuse reflectance spectrum of the adduct of Co(II) shows an absorption band at 17,937 cm^{-1} typical of Co(II) octahedra. In addition to this band, appreciable absorption is observed at 14275 cm^{-1}. Bands occurring at this frequency are generally associated with the presence tetrahedral Co(II) due to terminal tetrahedral units of octahedral short polymer chains. Similar phenomenon has been observed in the diffuse reflectance spectra of several octahedral polymeric Co(II) complexes. The ligand parameters for the Co(II) adduct were calculated according to Lever [14]. According to the number and position of the observed bands and considering the magnitude of the crystal field parameters as compared with that of Bolster [15], it is concluded that the adduct of Co(II) is pseudo-tetrahedrally surrounded in the terminal units by two bromine atoms and two oxygen atoms from two pyNO molecules and pseudo-octahedrally surrounded in the bridge-type structure by two bromine atoms and four oxygen atoms from four pyNO molecules [16,17]. The ligand field parameters for the adduct of Fe(II) were calculated according to Bolster [15]. It is concluded that the adduct of Fe(II) is pseudo tetrahedrally surrounded by three oxygen atoms from three molecules of pyNO and one bromine atom. For the adduct of Mn(II), since only forbidden bands can be observed in the electronic spectra of high-spin Mn(II) compounds, it is impossible to accurately determine the ligand-field parameters. It is, however, possible to deduce the local symmetry which is pseudo-tetrahedral

Table 3
Band maxima assignments and calculated ligand-field parameters for the compounds

Compound	ν_1 (cm^{-1})	ν_2 (cm^{-1})	ν_4 (cm^{-1})	ν_3 (cm^{-1})	Dq (cm^{-1})	B (cm^{-1})	Dq/B	β[a]
$[CoBr_2(pyNO)_3]_n$	8442[b]	17937[b]		23121[b]	949.5	700	1.356	0.721
		5590[c]		14275[c]	321	682	0.471	0.702
$NiBr_2(pyNO)_6$	8107[d]	12762[d]	14275[d]	23895[d]	811	585	1.386	0.568
$FeBr_2(pyNO)_3$	6912[e]				691.2			

Band maxima: $MnBr_2(pyNO)_3$, 22909 cm^{-1}; $CuBr_2(pyNO)_2$, 4850–12602 cm^{-1} (very broad band with no distinct maxima).
[a] $\beta = B/B_o$, $B_o = 971$ cm^{-1} (Co^{2+}) ([15]) = 1030 cm^{-1} (Ni^{2+}) ([15]).
[b] $\nu_1 = {}^4T_{2g} \leftarrow {}^4T_{1g}(F)$; $\nu_2 = {}^4A_{2g} \leftarrow {}^4T_{1g}(F)$; $\nu_3 = {}^2P, {}^2G, {}^4T_{1g}(P) \leftarrow {}^4T_{1g}(F)$.
[c] $\nu_2 = {}^4T_1(F) \leftarrow {}^4A_2$; $\nu_3 = {}^4T_1(P) \leftarrow {}^4A_2$.
[d] $\nu_1 = {}^3T_{2g} \leftarrow 3A_{2g}$; $\nu_2 = 3T_{1g}(F) \leftarrow 3A_{2g}$; $\nu_4 = {}^1E_g \leftarrow {}^3A_{2g}$; $\nu_3 = {}^3T_{1g}(P) \leftarrow {}^3A_{2g}$.
[e] $\nu_1 = {}^5T_2 \leftarrow {}^5E$.

Table 4
Enthalpies of dissolution at 298.15 K

Compound	Calorimetric solvent	No. of experiments	$\Delta_i H^\theta$ (kJ mol^{-1})
$MnBr_{2(s)}$	Methanol	5	-77.30 ± 2.62
$pyNO_{(s)}$	3:1 $MnBr_2$–methanol	5	29.14 ± 0.84
$[MnBr_2(pyNO)_3]_{(s)}$	Methanol	5	5.12 ± 0.25
$FeBr_{2(s)}$	Methanol	5	-46.04 ± 0.42
$pyNO_{(s)}$	3:1 $FeBr_2$–methanol	4	19.94 ± 0.57
$[FeBr_2(pyNO)_3]_{(s)}$	Methanol	5	27.33 ± 1.85
$CoBr_{2(s)}$	Methanol	4	-91.82 ± 1.21
$pyNO_{(s)}$	3:1 $CoBr_2$–methanol	4	24.09 ± 1.42
$[CoBr_2(pyNO)_3]_{(s)}$	Methanol	4	2.62 ± 0.05
$NiBr_{2(s)}$	Methanol	5	-23.60 ± 0.42
$pyNO_{(s)}$	6:1 $NiBr_2$–methanol	4	51.50 ± 0.89
$[NiBr_2(pyNO)_6]_{(s)}$	Methanol	4	50.20 ± 0.41
$CuBr_{2(s)}$	Methanol	5	-41.42 ± 1.26
$pyNO_{(s)}$	2:1 $CuBr_2$–methanol	4	18.77 ± 0.21
$[CuBr_2(pyNO)_2]_{(s)}$	Methanol	5	34.73 ± 1.00
$ZnBr_{2(s)}$	Methanol	5	-47.46 ± 1.14
$pyNO_{(s)}$	2:1 $ZnBr_2$–methanol	6	21.09 ± 0.85
$[ZnBr_2(pyNO)_2]_{(s)}$	Methanol	5	30.21 ± 0.75

[15], with Mn(II) surrounded by three oxygen atoms from three pyNO molecules and one bromine atom. For the Cu(II) adduct, the electronic spectrum show a single, rather broad band. Its intensity and position match those observed for pseudo-tetrahedral Cu(II) complexes [15].

3.4. Calorimetric measurements

The standard enthalpies of dissolution of metal(II) bromides, pyNO and adducts were obtained as previously reported [8]. The standard enthalpies of dissolution were obtained according with the standard enthalpies o reactions 1–4 in solution:

$$MBr_{2(s)} + \text{methanol} \rightarrow \text{solution A}; \quad \Delta_1 H^\theta \tag{1}$$

$$nL_{(s)} + \text{solution A} \rightarrow \text{solution B}; \quad \Delta_2 H^\theta \tag{2}$$

$$[MBr_2(pyNO)_n]_{(s)} + \text{methanol} \rightarrow \text{solution C}; \quad \Delta_3 H^\theta \tag{3}$$

$$\text{solution B} \rightarrow \text{solution C}; \quad \Delta_4 H^\theta \tag{4}$$

Table 4 gives the values obtained for all these dissolution enthalpies.

The application of Hess' law to the series of reactions 1–4 gives the standard enthalpies of the acid/base reactions ($\Delta_r H^\theta$) according to reaction 5:

$$MBr_{2(s)} + n\,pyNO_{(s)} \rightarrow [MBr_2(pyNO)_n]_{(s)}; \quad \Delta_r H^\theta = \Delta_1 H^\theta + \Delta_2 H^\theta - \Delta_3 H^\theta \tag{5}$$

Since the final state of reactions 2 and 3 is the same and $\Delta_4 H^\theta = 0$. Table 4 give the values obtained for the enthalpies of dissolution of metal(II) bromides ($\Delta_1 H^\theta$), pyNO in the solution of MBr_2 ($\Delta_2 H^\theta$) and of the adducts ($\Delta_3 H^\theta$). Uncertainty intervals given in this table are twice the standard deviation of the means of four or five replicate measurements. Combined errors were calculated from the square root of the sum of the square of the component errors.

From the values obtained for the standard enthalpies of the acid/base reactions ($\Delta_r H^\theta$) and by using appropriate thermochemical cycles [8,18,19], the following thermochemical parameters were determined: the standard enthalpies of formation ($\Delta_f H^\theta$), the standard enthalpies of decomposition ($\Delta_D H^\theta$), the standard lattice enthalpies ($\Delta_M H^\theta$) and the standard enthalpies of the Lewis acid/base reactions in the gaseous phase ($\Delta_r H(g)$). These latter values can be used to calculate the standard enthalpies of the M–O bonds [18], being equal to: $\bar{D}_{(M\text{–}O)} = -\Delta_r H^\theta(g)/n$. Tables 5 and 6 list the values obtained for all these thermochemical parameters.

For the determination of $\Delta_r H^\theta(g)$ it was necessary to assume that the molar standard enthalpies of sublimation of the adducts were equal to the enthalpy of sublimation of 1 mol of the ligand [21,22] as the melting points and thermal studies showed that the adducts decomposed on heating and were not found in the liquid phase and probably not in the gaseous phase. For some metal(II) bromides, there are not enough thermochemical data in the literature, e.g. the enthalpies of

Table 5
Auxiliary and calculated data (in kJ mol^{-1}) for metal(II) bromides and PyNO

Compound	$\Delta_f H^\theta$	$\Delta_s^g H^\theta$ or $\Delta_l^g H^\theta$
$MnBr_{2(s)}$	-384.9[a]	206[b]
$FeBr_{2(s)}$	-249.8[a]	204[a]
$CoBr_{2(s)}$	-220.9[a]	183[b]
$NiBr_{2(s)}$	-212.1[a]	170[b]
$CuBr_{2(s)}$	-141.8[a]	182.4[b]
$ZnBr_{2(s)}$	-328.65[a]	159.7[b]
$PyNO_{(s)}$	-77 ± 0.8[c]	81.9 ± 1.5[c]

[a] See [4].
[b] See text.
[c] See [20].

Table 6
Summary of the thermochemical results (in kJ mol^{-1}) for metal(II) bromide adducts

Compound	$\Delta_r H^\theta$	$\Delta_f H^\theta$	$\Delta_M H^\theta$	$\Delta_D H^\theta$	$\Delta_r H^\theta$(g)	$\bar{D}_{(M–O)}$
$[MnBr_2(pyNO)_3]_{(s)}$	−53.28 ± 2.76	−415.1 ± 4.2	−504.9 ± 5.7	229.0 ± 5.3	−423.0 ± 5.8	141.0 ± 1.9
$[FeBr_2(pyNO)_3]_{(s)}$	−53.43 ± 1.98	−280.1 ± 3.7	−503 ± 5	299.1 ± 4.9	−421 ± 6	140 ± 2
$[CoBr_2(pyNO)_3]_{(s)}$	−70.35 ± 1.87	−268.2 ± 3.6	−499 ± 5	316.1 ± 4.9	−417.5 ± 5.2	139.2 ± 1.7
$[NiBr_2(pyNO)_6]_{(s)}$	−22.30 ± 1.07	−188.2 ± 5.0	−684 ± 9	513.7 ± 9.1	−602 ± 9	100 ± 2
$[CuBr_2(pyNO)_2]_{(s)}$	−57.38 ± 1.62	−183.8 ± 3.1	−403.6 ± 3.6	221.2 ± 3.4	−321.7 ± 3.9	160.9 ± 2.0
$[ZnBr_2(pyNO)_2]_{(s)}$	−56.58 ± 1.61	−369.9 ± 3.1	−380.1 ± 3.9	220.4 ± 3.4	−298.2 ± 4.2	149.1 ± 2.1

formation in the gaseous phase are not cited. For these, the enthalpy values were estimated from the enthalpies of sublimation of a given metal(II) chloride by adding the difference between the enthalpies of sublimation of $FeCl_2$ and $FeBr_2$, or from the enthalpies of formation in the gaseous phase of $FeBr_2$ or $ZnBr_2$ by adding the difference between the enthalpies of formation in the gaseous phase of Fe or Zn with the considered metal. Table 7 presents the auxiliary data used for these calculations.

Based on the $\Delta_r H^\theta$ values for the adducts of the same stoichiometry, the acidity order of the salts can be obtained: $CuBr_2 > ZnBr_2$ and $CoBr_2 > FeBr_2 \cong MnBr_2$. Using the $\bar{D}_{(M–O)}$ values, the order is: $CuBr_2 > ZnBr_2$ and $MnBr_2 > FeBr_2 > CoBr_2$. The bond energy value found in the literature for $\bar{D}_{(Cu–O)}$ [24] in copper(II) pentane-2,4-dionate is 159±8 kJ mol^{-1}. The value found here is in good agreement with it. As a whole, the energies of the coordinate bonds form between pyNO and arsenic trihalides [25] are weaker than the bonds formed with transition metal(II) bromides.

The enthalpies for the process of hypothetical complex formation in the gaseous phase from metal(II) ions and pyNO can be evaluated:

$$M^{2+}_{(g)} + 2Br^{-}_{(g)} + n\text{pyNO}_{(g)} \rightarrow [MBr_2(\text{pyNO})_n]_{(g)}; \quad \Delta_{fI} H^\theta \tag{6}$$

with

$$\Delta_{fI} H^\theta = \Delta_f H^\theta(\text{adduct}_{(g)}) - \Delta_f H^\theta(M^{2+}_{(g)}) - 2\Delta_f H^\theta(Br^{-}_{(g)}) - n\Delta_f H^\theta(\text{pyNO}_{(g)})$$

Table 8 lists the values obtained for these enthalpy values. The environment around the M(II) ions is pseudo-tetrahedral in the case of Mn, Fe, Co, Cu or Zn as different atoms (oxygen and bromine) are present. Then, it is adequate to find correlations of the $\Delta_{fI} H^\theta$ rather than correlations of the $\bar{D}_{(M–O)}$ values. The correlation of the enthalpy changes of the ionic complex formation in the gaseous phase ($\Delta_{fI} H^\theta$) with the metal atomic number is present in Fig. 1. It shows part of the double periodic variation profile.

Table 7
Auxiliary data and enthalpy changes of the ionic complex formation process in the gaseous phase (kJ mol^{-1})

Compound	$\Delta_f H^\theta$
$FeCl_{2(s)}$ [a]	−341.79[b]
$Br^{-}_{(g)}$	−219.09[b]
$Mn^{2+}_{(g)}$	2522.0 ± 0.1[c]
$Fe^{2+}_{(g)}$	2751.6 ± 2.3[c]
$Co^{2+}_{(g)}$	2841.7 ± 3.4[c]
$Ni^{2+}_{(g)}$	2930.5 ± 1.5[c]
$Cu^{2+}_{(g)}$	3054.5 ± 2.1[c]
$Zn^{2+}_{(g)}$	2781.0 ± 0.4[c]
$Mn_{(g)}$	283.3[c]
$Fe_{(g)}$	416.3 ± 1.7[c]
$Co_{(g)}$	424.7 ± 2.6[c]
$Ni_{(g)}$	430.1[c]
$Cu_{(g)}$	338.9 ± 2.1
$Zn_{(g)}$	129.1 ± 0.4[c]

[a] $\Delta_s^g H^\theta = 193.3$ kJ mol^{-1} (see [4]).
[b] See [4].
[c] See [23].

Table 8
Auxiliary data and enthalpy changes of the ionic complex formation process in the gaseous phase (kJ mol^{-1})

Compound	$\Delta_f H^\theta$	$\Delta_r H^\theta$(g)	$\Delta_{fI} H^\theta$
$[MnBr_2(pyNO)_3]_{(g)}$	−333.2 ± 11.0	−423.0 ± 5.8	−2684.9 ± 14.5
$[FeBr_2(pyNO)_3]_{(g)}$	−198 ± 11	−421 ± 6	−2780 ± 12
$[CoBr_2(pyNO)_3]_{(g)}$	−187 ± 11	−417.5 ± 5.2	−2859 ±15
$[NiBr_2(pyNO)_6]_{(g)}$	−106 ± 21	−602 ± 9	−3136 ± 27
$[CuBr_2(pyNO)_2]_{(g)}$	−101.9 ± 7.6	−321.7 ± 3.9	−2897.5 ± 10.2
$[ZnBr_2(pyNO)_2]_{(g)}$	−288.0 ± 7.6	−298.2 ± 4.2	−2810.1 ± 10.0

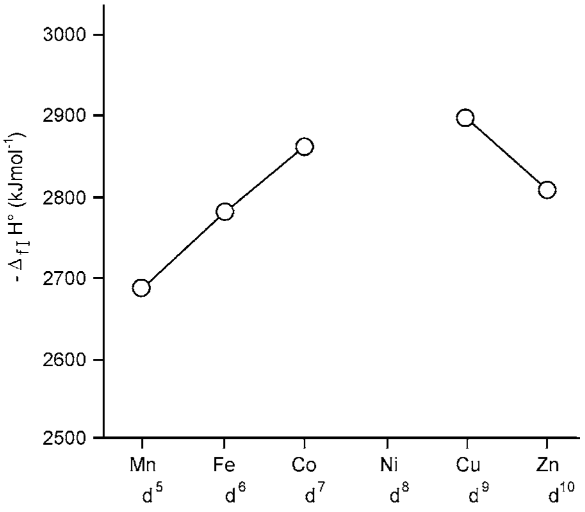

Fig. 1. Plot of enthalpy changes of complex formation in the gaseous phase from ionic components against *d*-electron configuration.

References

[1] J.V. Quagliano, J. Fujita, G. Franz, D.J. Phillips, J.A. Walmsley, S.Y. Tyree, J. Am. Chem. Soc. 83 (1961) 3770.
[2] R.L. Carlin, J. Am. Chem. Soc. 83 (1961) 3773.
[3] S. Kida, J.V. Quagliano, J.A. Walmsley, S.Y. Tyree, Spectrochim. Acta. 19 (1963) 89.
[4] D.D. Wagmam, W.H. Evans, V.B. Parker, R.H. Schumn, I. Halow, S.M. Churney, R.L. Nuttall, J. Phys. Chem. Ref. Data v(II) (1982) 2–50, 2–138, 2–139, 2–155, 2–166, 2–171, 2–177, 2–178, 2–191.
[5] E. Ochiani, J. Org. Chem. 18 (1953) 534.
[6] H.A. Flaschka, EDTA Titrations: An Introduction to Theory and Practice, Pergamon Press, second ed., London, 1964, p. 80–82, 85, 87–88.
[7] I.M. Kolthoff, E.B. Sandall, Tratado de Química Analítica Cuantitativa, Libreria y Editorial Nigar S. R. L., third ed., Buenos Aires, 1956, p. 371.
[8] P.O. Dunstan, Thermochim. Acta. 197 (1992) 201.
[9] E.F. Henrigton, Pure Appl. Chem. 40 (1974) 391.
[10] S. Kinda, J.V. Quagliano, J.A. Walmsley, S.Y. Tyree, Spectrochim. Acta. 19 (1963) 189.
[11] H. Wiley, S.C. Slaymaker, J. Am. Chem. Soc. 79 (1957) 2233.
[12] R.H. Shindo, Pharm. Bull. (Tokyo) 4 (1956) 460.
[13] J. Reedijk, P.W.N.M. Leeuwen, W.L. Groeneveld, Recueil 87 (1968) 129.
[14] A.B.P. Lever, J. Chem. Educ. 45 (1968) 711.
[15] M.W.G. Bolster, The Coordination Chemistry of Aminophosphine Oxides and Related Compounds, Thesis, Leiden, 1972, p. 83, 89, 95, 98, 100.
[16] A.B.P. Lever, J. Lewis, R.S. Nyholm, J. Chem. Soc. (1962) 1235.
[17] G. Yagupsky, R.H. Negrotti, R. Levitus, J. Inorg. Nucl. Chem. 27 (1965) 2603.
[18] P.O. Dunstan, Thermochim. Acta. 317 (1998) 165.
[19] P.O. Dunstan, L.C.R. dos Santos, Thermochim. Acta. 156 (1989) 163.
[20] M.L.C.P. da Silva, A.P. Chagas, C. Airoldi, J. Chem. Soc., Dalton Trans. (1988) 2113.
[21] A.P. Chagas, C. Airoldi, Polyhedron 8 (1989) 1093.
[22] P.O. Dunstan, Thermochim. Acta. 240 (1994) 91.
[23] H.A. Skinner, G. Pilcher, Q. Rev. Chem. Soc. 17 (1973) 264.
[24] R.J. Irving, M.A.V. Ribeiro da Silva, J. Chem. Soc., Dalton Trans. (1981) 99.
[25] P.O. Dunstan, Thermochim. Acta. 181 (1991) 143.